

## Stable vortex solitons in the two-dimensional Ginzburg-Landau equation

L.-C. Crasovan,<sup>1</sup> B. A. Malomed,<sup>2</sup> and D. Mihalache<sup>1</sup>

<sup>1</sup>*Department of Theoretical Physics, Institute of Atomic Physics, P.O. Box MG-6, Bucharest, Romania*

<sup>2</sup>*Department of Interdisciplinary Sciences, Faculty of Engineering, Tel Aviv University, Tel Aviv 69978, Israel*

(Received 19 June 2000; revised manuscript received 27 September 2000; published 20 December 2000)

In the framework of the complex cubic-quintic Ginzburg-Landau equation, we perform a systematic analysis of two-dimensional axisymmetric doughnut-shaped localized pulses with the inner phase field in the form of a rotating spiral. We put forward a qualitative argument which suggests that, on the contrary to the known fundamental azimuthal instability of spinning doughnut-shaped solitons in the cubic-quintic NLS equation, their GL counterparts may be stable. This is confirmed by massive direct simulations, and, in a more rigorous way, by calculating the growth rate of the dominant perturbation eigenmode. It is shown that very robust spiral solitons with (at least) the values of the vorticity  $S=0, 1$ , and  $2$  can be easily generated from a large variety of initial pulses having the same values of intrinsic vorticity  $S$ . In a large domain of the parameter space, it is found that all the stable solitons coexist, each one being a strong attractor inside its own class of localized two-dimensional pulses distinguished by their vorticity. In a smaller region of the parameter space, stable solitons with  $S=1$  and  $2$  coexist, while the one with  $S=0$  is absent. Stable breathers, i.e., both nonspiral and spiraling solitons demonstrating persistent quasiperiodic internal vibrations, are found too.

DOI: 10.1103/PhysRevE.63.016605

PACS number(s): 42.65.Tg, 47.32.Cc

### I. INTRODUCTION

Ginzburg-Landau (GL) equations constitute a class of universal models describing pattern formation in a great variety of nonlinear dissipative systems [1]. Among the patterns, localized pulses are especially interesting. While the theory of pulses in various one-dimensional (1D) models of the GL type was well elaborated [1–8], much less is known about two-dimensional (2D) localized patterns (“bright solitons”). In order to make the pulses stable, it is first of all necessary to stabilize the zero background (trivial solution to the equation), which can be done within the framework of the *cubic-quintic* (CQ) GL equation [2–4], or a model linearly coupling a cubic GL equation to a linear dissipative one [5].

Although the CQ GL equation was originally introduced by Sergeev and Petviashvili [2] in a 2D form, exactly in order to generate 2D localized pulses in the form of “spiral solitons,” much more work has been done to investigate not “solitons” of this type, but rather spiral waves extending to infinity [9,10]. In particular, the stability of delocalized spiral vortices in a model of a superflow, and interactions of vortices in a two-component GL system have been investigated in Refs. [11] and [12]. On the other hand, nonspiral *localized* 2D patterns were recently studied in other models, e.g., a complex Swift-Hohenberg equation [13].

The objective of this work is to develop a consistent analysis of spiral solitons, i.e., localized 2D objects with *internal vorticity*, which is characterized by an integer-valued “spin”  $S$ , within the framework of the complex CQ GL equation. A crucially important issue to be considered is the soliton’s stability at different values of  $S$ . Note that, in the dissipationless limit, the GL equation goes over into an equation of the nonlinear Schrödinger (NLS) type. Accordingly, a spiral soliton turns into a 2D soliton with an internal vorticity (ring vortex, or “spinning soliton”). However, a principal difference is that the GL equation may only have a few iso-

lated solitary-pulse solutions (normally, two, if one of them is expected to be stable, the second pulse playing the role of an unstable *separatrix* [5]), while its NLS counterpart, even if it is not integrable (which is definitely the case in the 2D situation), has a continuous family of soliton solutions, that may be parametrized by their energy. In the case when all the dissipative parameters of the GL model are small, i.e., it may be considered as a perturbation of its NLS counterpart, isolated pulses that survive as solutions to the GL equation are selected from the continuous family of the NLS solitons by a condition of the balance between the gain and losses [5].

The continuous family of the  $S=1$  soliton solutions to the two-dimensional CQ NLS equation was investigated in detail numerically in Ref. [14]. On the basis of simulations reported in Ref. [14], it had been concluded that the spinning solitons were stable, provided that their energy was large enough. However, we have recently found [15] that, in fact, these spinning solitons, as well as their counterparts in the form of “spinning light bullets” in the three-dimensional CQ NLS model [16], are subject to an azimuthal instability, which leads to their breakup into a set of fragments which are flying in tangential directions, each being a stable *non-spinning* soliton (the number of the fragments depends on the original spin and initial energy of the spinning soliton). Nonetheless, it has also been found that, in the case of large energies, when the soliton is a ring with small inner and large outer diameters (see, for example, Fig. 7 below), the instability is growing very slowly, thus explaining the robustness of the ring vortices reported in Ref. [14]. Moreover, this may also explain observation of an effectively *stable* spatial vortex soliton in a non-Kerr 3D optical medium reported in a recent experimental work [17]. It is also relevant to mention that, in contrast to this, 2D spinning solitons are very strongly unstable in a model with saturable nonlinearity (from which the CQ nonlinearity can be formally obtained as a truncated expansion) [18].

In the work [15], we have also performed an analytical

consideration of a particular mode of the instability of the spinning solitons in two- and three-dimensional CQ NLS equations, which is relevant just for the above-mentioned broad vortex rings with large energy. This particular instability mode is the spontaneous off-center displacement of the soliton's inner "bubble." It has been concluded that this mode gives rise to an instability of the solitons with  $S=1$  and 2, although it is not necessarily the fastest growing unstable mode. In direct simulations, this mode does not usually dominate the instability development; nevertheless, it can be observed in some cases (actually, in a 3D rather than 2D situation) [15].

Following the same line of arguments, one may expect that, on the contrary to the conservative NLS equation, in the GL model the vortex ring may be stable. Indeed, in the limit when the external size of the ring diverges, the vortex ring turns into a usual delocalized rotating spiral wave [10]. It is known that, generally, the latter wave in dissipative systems has a finite (nonzero) *stability margin* against the spontaneous off-center shift of its inner bubble. On the other hand, in the same limit the vortex ring in the NLS equation turns into a usual delocalized "optical vortex" (2D dark soliton) [19], which is, obviously, only *neutrally stable* against the spontaneous shift of the inner bubble. Therefore, the interaction of the inner bubble with the outer rim of the large-size but finite NLS soliton may destabilize the whole ring, turning the neutral shift mode into an unstable one, which is indeed the case in the CQ NLS equation [15]; however, the above-mentioned stability margin of the inner bubble against the shift inside the GL spiral wave may help to stabilize a *finite-size* spiral vortex too in the GL equation. Our simulations will show that it is indeed relatively easy to find a spiral soliton which is fairly stable against all the perturbations, including azimuthal ones which are fatal for the NLS vortex ring.

The rest of the paper is arranged as follows. The GL model is presented in detail in Sec. II, and in Sec. III we report results of extensive numerical simulations, separately for nonspiralizing and spiralizing solitons, with special emphasis on the test of the stability against azimuthal perturbations. Conclusions are formulated in Sec. IV.

## II. MODEL

We consider the (2+1)-dimensional CQ complex GL equation in a general form,

$$iA_z + i\delta \cdot A + (1/2 - i\beta)(A_{xx} + A_{yy}) + (1 - i\varepsilon)|A|^2A - (\nu - i\mu)|A|^4A = 0. \quad (1)$$

The equation is written in the "optical" notation, assuming evolution along the propagation coordinate  $z$  of a beam with the 2D cross section in the plane  $(x, y)$ . In fact, bulk (3D) optical media is the most appropriate system for experimental generation of vortex rings, see, e.g., Ref. [20]. In that case,  $A(x, y; z)$  is the local amplitude of the electromagnetic wave, the diffraction and cubic-self-focusing coefficients are normalized to be 1,  $\varepsilon$  is the cubic gain,  $\delta$  and  $\mu$  are the linear and quintic loss parameters (as a matter of fact, the

latter one accounts for the nonlinear gain saturation in optical media), and  $\nu$  is the quintic self-defocusing coefficient. Lastly,  $\beta$  is an effective diffusion coefficient (in optical media, diffusion takes place if light creates free charge carriers, which may take place, e.g., in semiconductor waveguides).

The "spiral solitons" are axisymmetric solutions to Eq. (1) of the form  $A(z, x, y) = U(z, r)\exp(iS\theta)$ , where  $r$  and  $\theta$  are polar coordinates in the  $(x, y)$  plane, and  $S$  is the above-mentioned integer "spin" (topological charge of the vortex). The complex amplitude  $U(z, r)$  obeys an equation

$$iU_z + i\delta \cdot U + (1/2 - i\beta)(U_{rr} + r^{-1}U_r - S^2r^{-2}U) + (1 - i\varepsilon)|U|^2U - (\nu - i\mu)|U|^4U = 0, \quad (2)$$

which is supplemented by boundary conditions stating that  $U \sim r^S$  at  $r \rightarrow 0$ , and  $U(r)$  decays exponentially at  $r \rightarrow \infty$ . Note that the localized solution can be interpreted as a *spiral soliton* because the function  $U(r)$  is complex,  $U(r) \equiv |U(r)|\exp(i\Phi(r))$ , hence equal-phase curves  $S\theta + \Phi(r) = \text{const}$  are spirals, rather than straight lines  $S\theta = \text{const}$ , as in the case of the CQ NLS equation, where  $U(r)$  is real [14, 21].

Our first purpose is to find stationary localized solutions to Eq. (2) which must be stable within the framework of this equation, i.e., they must be *attractors*, similarly to stable solitons in various forms of the 1D GL equation [4–7]. As the stability of the spiral solitons against the most dangerous azimuthal perturbations is not comprised by Eq. (2), it will be considered below separately.

It is relevant to mention that a stationary solution for a spiral soliton was sought for numerically already in the first work [2] in which the CQ GL model was introduced. However, a particular version of the model considered in that early work was very degenerate (with a single cubic nondissipative term in the equation), and stability of the spiral soliton was not really studied.

## III. NUMERICAL ANALYSIS

In order to find the solutions, we have performed numerical simulations of Eq. (2) at many different values of parameters and using various initial configurations  $U(z=0, r)$ . First, we will display typical examples of the formation of stable nonspinning and spinning (spiral) solitons, and then results of a very large number of simulations will be summarized in the form of a diagram showing regions of existence and nonexistence of different solitons in an appropriate parameter plane. Typical examples of stable breathers, both nonspinning and spinning, showing persistent quasiperiodic internal vibrations will be displayed too.

Before proceeding to the presentation of results, it is relevant to note that a positive quintic self-defocusing coefficient,  $\nu > 0$ , is necessary to prevent the wave collapse in the NLS counterpart of the GL equation (1). However, it is not ruled out that stable GL spiral solitons are possible with  $\nu = 0$ , or even if  $\nu$  takes small negative values, as the collapse might be prevented by the dissipative terms. Moreover, it is also possible that spiral solitons may exist with the opposite sign in front of the cubic self-focusing term in Eq. (1). Following the analogy with 1D models, we expect that the

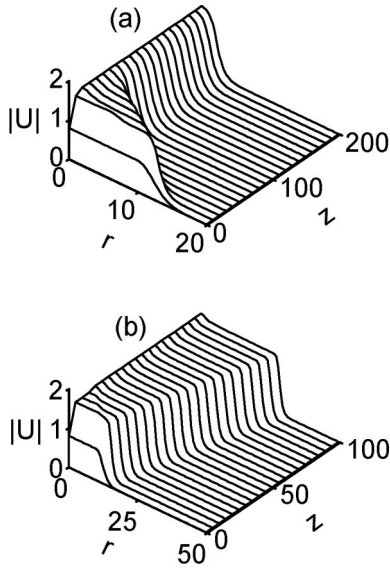


FIG. 1. (a) Formation of the nonspinning ( $S=0$ ) two-dimensional soliton at  $\beta=0.5$ ,  $\delta=0.5$ ,  $\nu=0.1$ ,  $\mu=1$ , and  $\varepsilon=2.5$ . (b) Formation of a continuous wave for the same parameters as in the panel (a) but with a different nonlinear gain,  $\varepsilon=2.6$ . The initial field is real,  $U(r; z=0)=0.8$  for  $r \leq 10$ , and  $U(r; z=0)=0.8 \exp[-(r-10)^2/9]$  for  $r > 10$ .

solitary pulse would have a much larger internal phase *chirp* in the latter case, which is, obviously, very important just for the spiral solitons. However, these issues are left beyond the scope of the present work.

### A. Zero-spin solitons

At first, we consider zero-spin (non-spiral) 2D stationary solutions with  $S=0$  (in the CQ NLS equation, such solutions were recently studied in detail in Ref. [22]). Our simulations have demonstrated that quite arbitrary initial pulses easily self-trap into (are *attracted* by) a stationary solution, which is similar to a “plain pulse” numerically found in Ref. [7] in the 1D model. As a typical example, the formation of a stationary pulse from a very broad input at  $\beta=0.5$ ,  $\delta=0.5$ ,  $\nu=0.1$ ,  $\mu=1$ , and  $\varepsilon=2.5$  is displayed by Fig. 1(a), while Fig. 1(b) shows the evolution of the same input for a slightly larger nonlinear gain,  $\varepsilon=2.6$ . One can see that in the latter case a stationary pulse is not formed; instead, the structure expands indefinitely, generating an advancing front similar to a 1D structure investigated in detail in Ref. [7]. A transition, with the increase of the cubic gain, from solitons to spatially uniform continuous waves (cw) extending to infinity is a natural feature, that can be easily explained in 1D by means of the perturbation theory [3,4]. Thus, for the above-mentioned set of parameters, a critical value of the gain  $\varepsilon$  separating the localized and cw states is between 2.5 and 2.6.

As it was mentioned in the Introduction, the formation of a stationary pulse is a result of the balance between the gain and losses. Figure 1 and many other simulations not shown here demonstrate that the balance is sensitive to the size of the gain and loss coefficients. In particular, the formation of a stable pulse or cw (the two outcomes shown in Fig. 1) is

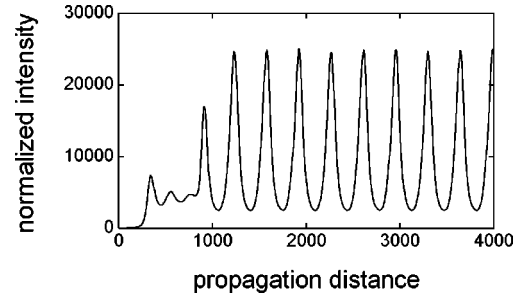


FIG. 2. Quasiperiodic evolution of the squared amplitude (intensity) of a nonspinning vibrating soliton at  $\beta=0.05$ ,  $\delta=0.05$ ,  $\nu=2$ ,  $\mu=0.2$ , and  $\varepsilon=0.3$ . The initial field is  $U(r; z=0)=(0.88/\sqrt{2})\exp[-(r/6)^2]$ .

not the only possible result. At some values of the parameters, breathers, i.e., localized pulses with persistent internal vibrations, similar to those discovered in various 1D GL models [6], were found too. An example of the breather with a huge amplitude of the intensity oscillations is presented in Fig. 2. At quasiperiodically repeating values of  $z$  corresponding to the minimum intensity, the pulse is found to be very broad and flat.

### B. Spinning solitons

We were able to find stable localized solutions to Eq. (2) in a systematic way for spinning (spiral) solitons with  $S=1$  and  $S=2$  (we did not consider higher values of the spin). Typical examples of the formation of spiral solitons for these two cases are shown in Fig. 3. In particular, in the case  $S=2$ , this resembles formation of the “composite pulse,” which was found to be stable in the 1D GL model studied in Ref. [7]. However, a direct analog of the “composite pulse” in the present (2+1)D model has never been found.

The spinning solitons, as well as the nonspinning ones considered above, are found to be strong attractors, as they

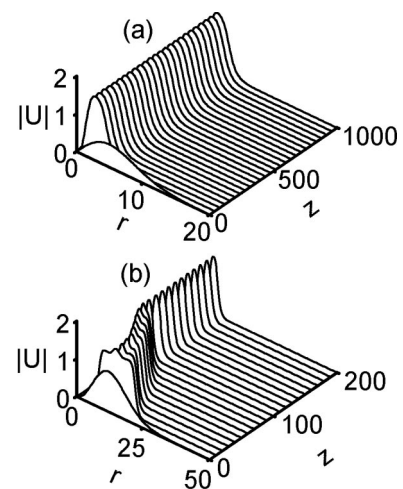


FIG. 3. Formation of spinning solitons from real initial field configurations: (a)  $S=1$  and (b)  $S=2$ . The parameters are  $\beta=0.5$ ,  $\delta=0.5$ ,  $\nu=0.1$ ,  $\mu=1$ , and  $\varepsilon=2.5$ . The initial field distributions are: (a)  $U(r; z=0)=0.2r \exp[-(r/7)^2]$ , and (b)  $U(r; z=0)=0.02r^2 \exp[-(r/12)^2]$ .



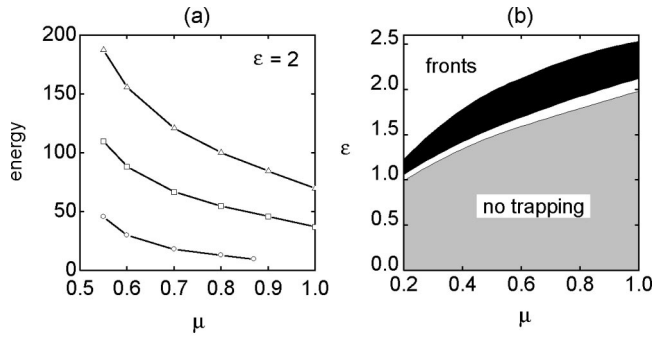


FIG. 4. (a) The integral power  $I$  versus quintic loss  $\mu$  for a fixed cubic gain  $\epsilon=2$ . The other parameters are  $\beta=0.5$ ,  $\delta=0.5$ , and  $\nu=0.1$ . The circles, squares, and triangles correspond to, respectively, nonspinning solitons, spinning solitons with  $S=1$ , and spinning ones with  $S=2$ . (b) The existence domain in the parameter plane  $(\epsilon, \mu)$  for both spinning and nonspinning stable solitons. The other parameters are:  $\beta=0.5$ ,  $\delta=0.5$ , and  $\nu=0.1$ .

can be generated from a large variety of inputs. Another important finding is that stable solitons with all the three values of the vorticity considered here,  $S=0,1,2$ , coexist in a large domain of the parameter space, see details below (we will also display a smaller region of the parameter space, in which stable solitons with  $S=1$  and  $S=2$  coexist, while zero-spin solitons were not found). In other words, each soliton is a strong attractor inside its own class of pulses, distinguished by the value of the spin, which plays the role of a *topological invariant*.

An important characteristic of solitons is their *integral power*, which is defined in the usual way, as  $I=2\pi\int_{-\infty}^{+\infty}|U(r)|^2rdr$ . The power has been found to take very different values for the coexisting solitons with different values of the spin. This is illustrated by Fig. 4(a), where the power is shown as a function of the nonlinear quintic loss parameter  $\mu$ . Similar relations between powers of solitons with different values of the spin were also found in the two- and three-dimensional CQ NLS equations [21].

To proceed from the typical examples displayed above to the presentation of systematic results, in Fig. 4(b) we display the existence domains for both spinning and nonspinning solitons in the parameter plane  $(\epsilon, \mu)$ . In the black region, there exist both spinning and nonspinning stable solitons, whereas in the lower white strip *only spinning* solitons have been found to form. In the gray region, solitons do not form at all. Lastly, in the upper white region, initial pulses have been found to expand indefinitely, generating the above-mentioned fronts.

Typical radial profiles of the solitons with  $S=0, 1$ , and  $2$  are displayed in Fig. 5. One can see from this figure that the inner radius of the spinning solitons quite naturally increases with the spin.

In other regions of the parameter space we have found apparently stable *spinning breathers* with  $S=1$  and  $S=2$ , which demonstrate persistent quasiperiodic internal vibrations. Figure 6 presents an example of a spinning breather with  $S=1$ . Note that the quasiperiodic oscillations are very similar to those observed for the nonspinning case (see Fig. 2). We mention that the nonspiraling ( $S=0$ ) and spiraling

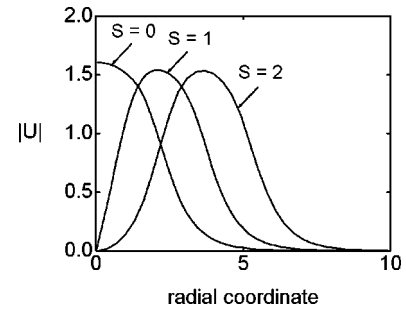


FIG. 5. Radial profiles of the spinning and nonspinning solitons at  $\beta=0.5$ ,  $\delta=0.5$ ,  $\nu=0.1$ ,  $\mu=1$ , and  $\epsilon=2.5$ .

( $S=1,2$ ) breathers coexist with each other at the same values of the parameters, whereas the stationary (nonvibrating) solitons do not form for those parameter values.

### C. Azimuthal stability

As it was explained above, the comparison with the spinning solitons in the CQ NLS model strongly suggests that overall stability of the solitons is determined by azimuthal perturbations breaking the axial symmetry of the solutions. Recall that the reduced equation (2) employed above cannot include azimuthal perturbations. Therefore, in order to test this kind of the stability, we have simulated the full equation (1) directly in the Cartesian coordinates. Doing this, we have found that both nonspinning and spiral solitons found above from Eq. (2) are remarkably *stable* against azimuthal perturbations, in accordance with the qualitative arguments presented in the Introduction. The stable existence of the solitons was verified, simulating their propagation over a huge distance, up to  $z=4000$ .

Although large-scale simulations of the full underlying equation are quite sufficient to predict observation of stable solitons in experiments, this does not provide for a mathematically complete evidence of the solitons' stability. A direct way to prove the true stability is to consider the eigenvalue problem produced by the linearization of the evolution equation around the corresponding stationary solutions. We have performed this analysis too, aiming to compute the largest growth rates (eigenvalues) of the azimuthal perturbation eigenmodes for different values of the perturbation in-

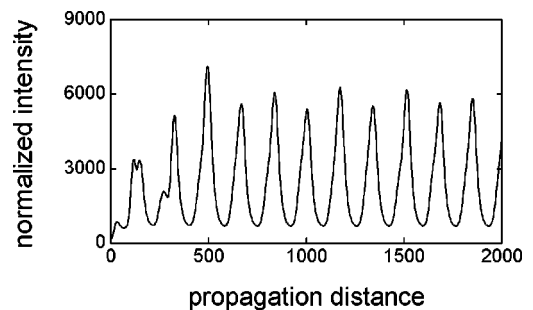


FIG. 6. Quasiperiodic evolution of the squared amplitude (intensity) of a vibrating spinning soliton with  $S=1$  for the same values of the parameters as in Fig. 2. The initial field is  $U(r; z=0) = (0.25/\sqrt{2})r \exp[-(r/9)^2]$ .

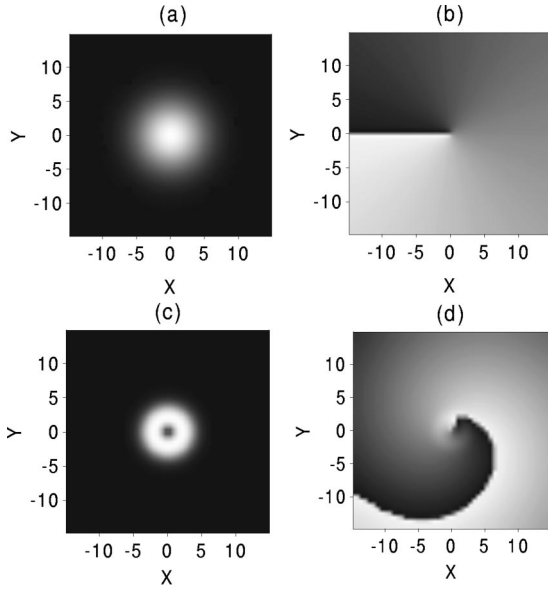


FIG. 7. Gray-scale plots of the input Gaussian field with the vorticity  $S=1$ : (a) amplitude and (b) phase. The output field at  $z=150$ : (c) amplitude and (d) phase. The parameters are  $\beta=0.5$ ,  $\delta=0.5$ ,  $\nu=0.1$ ,  $\mu=1$ , and  $\varepsilon=2.5$ .

dex  $n$  (which is independent from the spin  $S$  of the stationary solution in question). The numerical procedure we have used in order to obtain the growth rate of the dominant perturbation eigenmode is described in detail in Refs. [18] and [23–25].

In *all the cases* when the direct simulations produced apparently stable stationary solitons, we have found that the largest growth rate of the perturbation eigenmodes has a *negative* real part, thus corroborating the stability of the corresponding stationary solitons. For example, the real parts of the largest growth rate of the perturbation eigenmodes for the spiral soliton with  $S=1$  whose formation is shown in Fig. 3(a) are  $\text{Re } \lambda = -0.0005$ ,  $-0.185$  and  $-0.221$  for the perturbation indices  $n=1, 2$ , and  $3$ , respectively. The fact that the real part of the largest growth rate is clearly negative, rather than being equal to zero, is a consequence of the dissipative nature of the GL equation, as it was explained in the Introduction.

Lastly, to assess the range in the space of the initial configurations for which the stable solitons are attractors, we have additionally performed a large number of direct simulations with initial pulses in the form of Gaussians with intrinsic vorticity. In all the cases in which the existence of stable spiral solitons was known, the initial Gaussians rapidly developed into them, keeping the initial value of the spin. To illustrate this, in Figs. 7(a) and 7(b) we display gray-scale plots representing the amplitude and phase of the initial Gaussian beam, which was taken as

$$A(x,y;z=0) = 1.6 \exp[-(x^2+y^2)/25] \cdot \exp(i\theta)$$

(i.e., it has  $S=1$ ), whereas in Figs. 7(c) and 7(d) the amplitude and phase of the established doughnut-shaped soliton are shown at  $z=150$ .

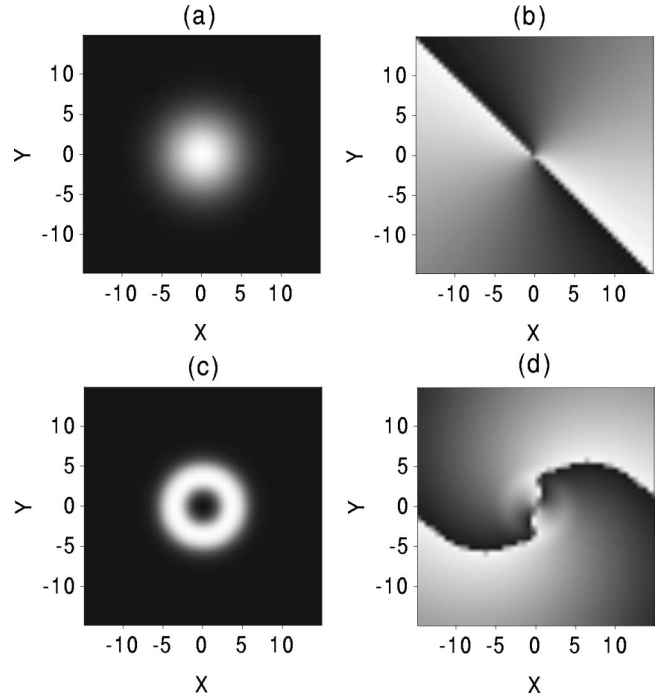


FIG. 8. The same as in Fig. 6, but for the vorticity  $S=2$ . The output field was taken at  $z=200$ .

The same initial intensity distribution, but with  $S=2$ , i.e.,

$$A(x,y;z=0) = 1.6 \exp[-(x^2+y^2)/25] \cdot \exp(2i\theta),$$

easily generates a stable spiral soliton with  $S=2$ , as it is seen in Fig. 8. Naturally, the  $S=2$  soliton has an essentially larger size of its inner “bubble,” cf. Fig. 5. The output displayed in Fig. 8 was taken at  $z=200$ , although, in fact, the formation of the soliton completed itself at the propagation distance  $z \sim 50$ .

Lastly, we note that the phase plots corresponding to the established solitons displayed in Figs. 7(d) and 8(d) clearly show a spiral structure, justifying the application of the term “spiral solitons” to the 2D solitary-wave patterns considered in this work.

#### IV. CONCLUSIONS

In the framework of the complex cubic-quintic Ginzburg–Landau equation of a general form, we have developed a systematic analysis of two-dimensional axisymmetric doughnut-shaped localized pulses with the inner phase field in the form of rotating spirals. We have put forward a qualitative argument which suggests that, on the contrary to the known azimuthal instability of spinning doughnut-shaped solitons in the cubic-quintic NLS equation, their GL counterparts may be stable. This is confirmed by many direct numerical simulations, the results of which have been summarized in the form of a diagram showing regions of existence and nonexistence of the spiraling and nonspiraling solitons in an appropriate parameter plane. Robustness of the solitons with the values of the intrinsic spin 0, 1, and 2, strongly suggested by direct simulations, was rigorously con-

firmed by computation of the largest growth rate for eigenmodes of azimuthal perturbations. For solitons found to be stable in direct simulations, the largest growth rate was always found to have a negative real part. In addition, we have shown that very robust spiral solitons with (at least)  $S=0$ , 1, and 2 can be easily generated from rather arbitrary localized inputs having the same internal vorticity. Moreover, in a large domain of the parameter space, both nonspinning and spinning solitons have been found to coexist, each one being a strong attractor inside its own class of pulses distinguished by the integer value of the vorticity. In a small region of the parameter space, the stable solitons with  $S=1$  and  $S=2$  have been found to coexist, while nonspiraling ones (with  $S=0$ ) are absent. In addition to that, in regions of the parameter space where stable solitons do not form, apparently stable breathers, both nonspiraling and spiraling, have been found to coexist with each other.

A challenging problem is the interaction between spiral solitons with equal or different vorticities (interactions between spirals extending to infinity have been already studied in detail by means of analytical and numerical methods [10]). If the solitons are far separated, and their vorticities are equal or opposite, the interaction can be described analytically in terms of an effective potential, using technique elaborated in Ref. [26]. However, in the most interesting case when the solitons are essentially overlapped and, hence, they interact strongly, direct simulations are necessary.

#### ACKNOWLEDGMENTS

We appreciate valuable discussions with L. M. Pismen, N. N. Akhmediev, and J. M. Soto-Crespo.

- 
- [1] M. C. Cross and P. C. Hohenberg, *Rev. Mod. Phys.* **65**, 851 (1993).
- [2] A. M. Sergeev and V. I. Petviashvili, *Dokl. Akad. Nauk SSSR* **276**, 1380 (1984) [*Sov. Phys. Dokl.* **29**, 493 (1984)].
- [3] B. A. Malomed, *Physica D* **29**, 155 (1987) (see Appendix in this paper); O. Thual and S. Fauve, *J. Phys. (Paris)* **49**, 1829 (1988).
- [4] W. van Saarloos and P. Hohenberg, *Phys. Rev. Lett.* **64**, 749 (1990); V. Hakim, P. Jakobsen, and Y. Pomeau, *Europhys. Lett.* **11**, 19 (1990); B. A. Malomed and A. A. Nepomnyashchy, *Phys. Rev. A* **42**, 6009 (1990).
- [5] B. A. Malomed and H. G. Winful, *Phys. Rev. E* **53**, 5365 (1996); J. Atai and B. A. Malomed, *ibid.* **54**, 4371 (1996); *Phys. Lett. A* **246**, 412 (1998).
- [6] H. R. Brandt and R. J. Deissler, *Phys. Rev. Lett.* **63**, 2801 (1989); R. J. Deissler and H. R. Brandt, *ibid.* **72**, 478 (1994); **74**, 4847 (1995); **81**, 3856 (1998); H. Sakaguchi and B. A. Malomed, *Physica D* **147**, 273 (2000).
- [7] V. V. Afanasjev and N. Akhmediev, *Opt. Lett.* **20**, 1970 (1995); V. V. Afanasjev, N. Akhmediev, and J. M. Soto-Crespo, *Phys. Rev. E* **53**, 1931 (1996).
- [8] L.-C. Crasovan, B. Malomed, D. Mihalache, and F. Lederer, *Phys. Rev. E* **59**, 7173 (1999).
- [9] P. Couillet, L. Gil, and D. Repaux, *Phys. Rev. Lett.* **62**, 2957 (1989).
- [10] L. M. Pismen, *Vortices in Nonlinear Fields* (Oxford University Press, Oxford, 1999).
- [11] I. Aranson and V. Steinberg, *Phys. Rev. B* **53**, 75 (1996).
- [12] I. S. Aranson and L. M. Pismen, *Phys. Rev. Lett.* **84**, 634 (2000).
- [13] V. B. Taranenko, K. Staliunas, and C. O. Weiss, *Phys. Rev. Lett.* **81**, 2236 (1998); V. J. Sanchez-Morcillo and K. Staliunas, *Phys. Rev. E* **60**, 6153 (1999).
- [14] M. Quiroga-Teixeiro and H. Michinel, *J. Opt. Soc. Am. B* **14**, 2004 (1997).
- [15] B. A. Malomed, L.-C. Crasovan, and D. Mihalache (unpublished).
- [16] D. Mihalache, D. Mazilu, L.-C. Crasovan, B. A. Malomed, and F. Lederer, *Phys. Rev. E* **61**, 7142 (2000).
- [17] A. G. Truscott, M. E. J. Friese, N. R. Heckenberg, and H. Rubinsztein-Dunlop, *Phys. Rev. Lett.* **82**, 1438 (1999).
- [18] W. J. Firth and D. Skryabin, *Phys. Rev. Lett.* **79**, 2450 (1997).
- [19] C. T. Law and G. A. Swartzlander, *Opt. Lett.* **18**, 586 (1993).
- [20] D. V. Petrov, L. Torner, J. Martorell, R. Vilaseca, J. P. Torres, and C. Cojocar, *Opt. Lett.* **23**, 1444 (1998).
- [21] A. Desyatnikov, A. Maimistov, and B. A. Malomed, *Phys. Rev. E* **61**, 3107 (2000).
- [22] M. Quiroga-Teixeiro, A. Berntson, and H. Michinel, *J. Opt. Soc. Am. B* **16**, 1697 (1999).
- [23] N. N. Akhmediev, V. I. Korneev, Yu. V. Kuz'menko, *Zh. Eksp. Teor. Fiz.* **88**, 107 (1985) [*Sov. Phys. JETP* **61**, 62 (1985)]; J. M. Soto-Crespo, D. R. Heatley, E. M. Wright, and N. N. Akhmediev, *Phys. Rev. A* **44**, 636 (1991); J. Atai, Y. Chen, and J. M. Soto-Crespo, *Phys. Rev. A* **49**, R3170 (1994).
- [24] D. E. Edmundson, *Phys. Rev. E* **55**, 7636 (1997).
- [25] L. Torner and D. V. Petrov, *Electron. Lett.* **33**, 608 (1997); D. V. Petrov and L. Torner, *Opt. Quantum Electron.* **29**, 1037 (1997); D. V. Skryabin and W. J. Firth, *Phys. Rev. E* **58**, 3916 (1998).
- [26] B. A. Malomed, *Phys. Rev. E* **58**, 7928 (1998).